Amplifier similariton fiber laser with a hybrid-mode-locking technique

XINYANG LIU,[1,*] MIKKO NÄRHI,[1] DMITRY KOROBKO,[2] AND REGINA GUMENYUK[1]

[1] *Laboratory of Photonics, Tampere University, Korkeakoulunkatu 3, Tampere 33720, Finland*
[2] *Ulyanovsk State University, 42 Leo Tolstoy Street, Ulyanovsk 432017, Russia*
*xinyang.liu@tuni.fi

Abstract: By employing both frequency shifting and nonlinear polarization rotation mechanisms in a Yb-doped fiber laser, similariton operation regime is demonstrated. Directly generated pulses from an oscillator has a duration of 7.8 ps with 20.5 nm spectrum width and average output power of 7.4 mW with a repetition rate of 26.4 MHz. The pulses can be externally dechirped to be 140 fs. Through numerical simulations we illustrate the details of similariton pulse formation under the simultaneous action of two mode-locking techniques and advantages of hybrid mode-locking approach.

1. Introduction

As a golden model for nonlinear systems, generalized nonlinear Schrödinger equation (GNLSE) has been applied in various branches of physics and applied mathematics, including fluid dynamics, nonlinear quantum field theory, optics, theory of turbulence and phase transitions [1,2]. Particularly in ultrafast optical pulse generation in fiber laser, GNLSE has been utilized to predict and study generation of different types of optical wave packets, e.g. conventional soliton [3], dispersion-managed (DM) soliton [4], dissipative soliton in all-normal dispersion (ANDi) cavity [5] and similariton [6,7]. In shaping of these pulses, dominance of different mechanisms has been identified. Balance of nonlinearity and dispersion results in formation of conventional solitons. By engineering dispersion map and energy dissipation of the cavity, the last three types of solitons can be obtained [8,9]. Observation sequence of those soliton counterparts follows a route of gradually enhanced maximum pulse energy and peak power, which are essentially limited by nonlinearity induced pulse distortion or wave-breaking [9], being especially pronounced in laser cavity with anomalous-dispersion components. The latest discovered amplifier similariton, an asymptotic solution of GNLSE with gain and normal dispersion, features distinctively parabolic pulse profile and linear frequency chirp through pulse, which grant amplifier similariton ability of tolerating high nonlinearity and consequent property of wave-breaking free [9]. Because linear chirp through pulse can be compensated by dispersive components like grating pairs, this makes amplifier similariton pulses highly attractive for fiber laser systems that are based on chirped pulse amplification (CPA) technique, possibly enabling delivery of high-peak-power Fourier transform-limited pulses without sidelobes at the output. In recent years, the researchers have demonstrated advances of similariton fiber lasers in different aspects. Chunyang *et al.* [10] investigated tunability of a self-similar Yb-doped fiber laser and realized similariton operation from 1030 nm to 1100 nm with sub-100 fs pulse duration. Uğur *et al.* demonstrated a spatiotemporal mode-locked self-similar Yb-doped fiber laser using multimode fiber. Average output power was scaled to 90 mW and pulse duration can be dechirped to 192 fs [11].

By sending a pulse of any shape to normal dispersion fiber with gain, it will gradually evolve to a parabolic pulse, whose characteristic is only determined by the initial pulse energy and fiber parameters [12]. During further propagation in fiber with normal dispersion, the pulse

maintains its parabolic pulse shape and a linear chirp, while both spectral and temporal widths exponentially broaden with distance, potentially endowing the similariton ability to have wide spectral bandwidth, consequently, short pulse duration can be obtained [13]. However spectral and temporal broadenings require compensation to maintain a stable self-similar evolution in the cavity, which has been proven to be a challenging task [14]. To provide necessary compensation of the spectral/pulse broadening, several solutions were proposed and successfully realized in the mode-locked fiber lasers. In cavity with the dispersion map a long segment of anomalous dispersion fiber allows pulse duration to be compressed and stabilizes spectral width [14]. In all-normal dispersion fiber laser pulses are shortened in both time and frequency domains by placing a narrow-band filter in cavity [15].

Even though the gain fiber as a nonlinear attractor plays a main role in similariton pulse formation, saturable absorption is still important in stabilizing pulses, which occurs through suppression of low-intensity instabilities. Nonlinear polarization rotation (NPR) as an effective saturable absorption mechanism has been applied in many mode-locking lasers. The shortest pulses to date from fiber laser were obtained from the cavity with self-consistent similariton evolution employing NPR mode-locking [16]. However, NPR is subject to environmental perturbation and requires adjustment from time to time to maintain laser operation.

To further support stable self-similar evolution in the cavity, we propose to use a hybrid approach incorporating NPR and frequency shifting. NPR results in establishment of pulse operation whereas a small frequency shift of 69.46 MHz leads to efficient filtering of low-intensity CW signal and vanishing undesirable perturbations in the cavity. This technique enables to achieve a stable similariton pulse even with non-optimum NPR parameters. We demonstrate a Yb-doped mode-locked fiber laser generating 7.8 ps similariton pulses with 20.5 nm spectrum bandwidth. The pulses are further compressed down to 140 fs using a grating pair. The experimental work is supported by numerical modelling yielding the insight of hybrid mode-locking operation in the amplifier similariton fiber laser.

2. Principle of frequency shifting for mode-locking

A frequency shifter, whose function in the cavity is to continuously add a small frequency shift (up or down) onto incident light, can discriminate high-peak-power pulse radiation and low-intensity continuous wave (CW) radiation in the frequency domain with help of a spectral filter. This is illustrated in Fig. 1.
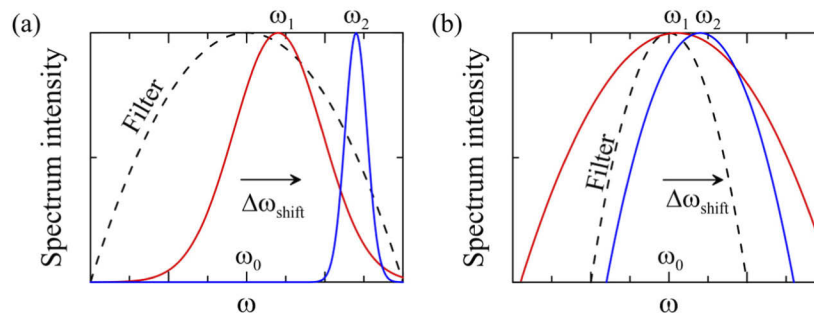

Fig. 1. The principle of frequency shifting operation in the mode-locked fiber laser incorporating intracavity filter. (a) FSF mode-locking scheme for the pulsed regime characteristic to conservative, DM and dissipative solitons formed in ANDi laser; (b) the FSF-mode-locking scheme with similariton amplifier laser specific. Red line indicates a broadband pulse's spectrum arriving to the frequency shifter, blue line –a narrow band spectrum, the dashed line is a filter's spectral profile.

The realization of any mode-locking technique is possible only in the cavity with positive feedback, i.e., the greater intensities must undergo lower losses. In the case of NPR mode-locking, appropriate selection of orientation of polarization controllers and polarizers leads to increase of cavity transmission with an increase of peak power of pulses or pulse narrowing as well as effective discrimination of broadband and narrowband spectra [17,18]. Positive feedback in the case of frequency shifted feedback (FSF) mode-locking is formed when the generated pulse passes through frequency shifter and subsequent bandpass filter (Fig. 1(a)) [19–23]. Under the influence of the frequency shifter, the pulse spectrum is displaced from the center of the filter, however, the filter induces a reverse shift of spectrum center due to attenuation of edge spectral components, and amount of this shift is proportional to filter slope and to the square of pulse spectrum width [23]. As a consequence, a situation arises that corresponds to a positive feedback - a pulse with a wide spectrum experiences less loss, because its carrier frequency ω_1 is shifted closer to the centre of the filter ω_0 than a narrowband pulse at a frequency ω_2 (Fig. 1). Apart from that, pulses with wider spectrum/higher intensity can induce more spectrum broadening through self-phase modulation (SPM) to compensate frequency shift effect than CW signal and narrowband/low intensity pulses. Eventually, the CW signal and narrowband pulses are filtered, and their energy is transferred to the broadband pulse. This is very efficient process which can lead to formation of highly environmentally stable pulsed regime in the cavity [24,25].

The growth of the energy and, accordingly, the spectrum widths are limited by negative feedback that occurs when the spectrum width reaches a certain limiting value. Filtering leads to the fact that, with a further increase in pumping, the generation of new pulses becomes more energetically favourable for the laser, rather than broadening of the spectrum of an individual pulse. The negative feedback is also general effect and applicable to NPR technique as well [26,27].

In earlier works investigating pulse generation by frequency shifter and filter, the balance of the pulse parameters was studied upon their minor changes during passage through the resonator [28,29]. In case of a similariton laser, the pulse parameters undergo a significant change along cavity. Pulses before filter have a spectral width several times (typically more than 5 [30]) wider than filter bandwidth (Fig. 1 (b)). The effect of reverse shift induced by the filter is enhanced significantly, and the discrimination of transmissions between high-intensity pulses and low-intensity pulses of different intensities decrease. For FSF mode-locking it means to support the pulse with broadband spectrum it requires to apply a large frequency shift, which is not realistic (it will be discussed in the details in the section 5). We should note that despite an increase of reverse shift for broadband pulses, the positive feedback continues to be strong and effective for narrow band pulses or low-intensity CW propagated in the same cavity. The role of FSF mode-locking and its potential effectiveness in this situation has remained open until now. So, one of the goals of this work was to study the possibility of using FSF mode-locking in a similariton laser.

3. Experimental setup

Experimental setup is shown in Fig. 2. ~1 m single-mode Yb-doped fiber (YDF) with 400 dB/m absorbance at 980 nm is employed to provide gain. The ring cavity is closed by ~6 m single-mode passive fiber and 32 cm free space incorporating an acousto-optic tunable filter (AOTF). Two diode lasers operating at 980 nm are utilized to pump YDF from both ends through two wavelength-division multiplexers (WDM). The optical power is extracted from the cavity via 22% output coupler. A polarization-independent isolator ensures counter clockwise operation. The AOTF is driven by a signal generator at 69.46 MHz and has a transmission bandwidth of ~4 nm with a central wavelength of 1030 nm and works as a versatile device to provide both spectral filtering and frequency shifting effects. The transmittance profile of AOTF is measured by using amplified spontaneous emission (ASE) from YDF as shown in Fig. 3. Side lobes near

main peak result from intrinsic property of Bragg diffraction [31]. One pair of lenses are used to optimize the free space light coupling. After AOTF, first-order diffracted light that is horizontally linearly polarized and frequency shifted is coupled into following fiber. It is noteworthy that coupling loss from free space to fiber is ~90%. This can be attributed to light beam quality is degraded after being diffracted. This large loss contributes to cavity dissipation, which is essential to the formation of a similariton [32]. A polarization controller (PC) applied to YDF controls polarization state. Setting total pump power at 869 mW and carefully adjusting the PC, the laser can run into a stable mode-locking regime with an average output power of 7.4 mW.
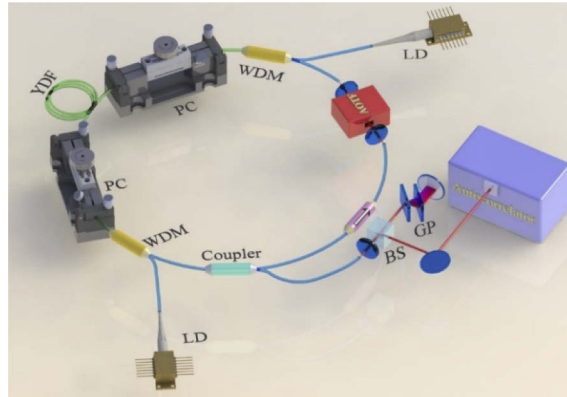

Fig. 2. Schematic of the similariton laser. LD, laser diode; YDF, Yb-doped fiber; PC, polarization controller; WDM, wavelength-division multiplexer; AOTF, acousto-optic tunable filter, BS, beam splitter; GP, grating pair.
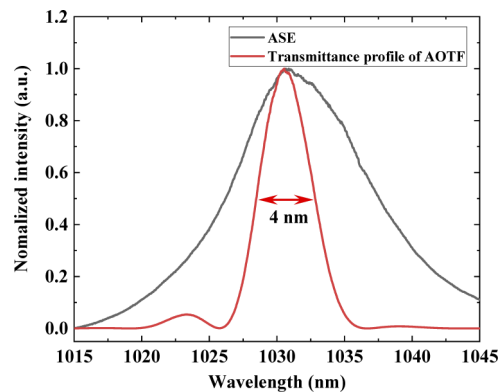

Fig. 3. Normalized ASE intensity (black line) and transmittance profile of AOTF (red line).

4. Experimental results and discussion

Laser performance is summarized in Fig. 4. The output pulse train is monitored by a fast photodiode (DET01CFC, 1 GHz) associated with an oscilloscope (DSO9254A, 2.5 GHz) and one typical recording is shown in Fig. 4(a). Output spectrum has a 20.5 nm full-width-at-half-maximum (FWHM) with associated spectrum presented in Fig. 4(b). The spectrum has a typical profile of similariton pulses with smooth edges and curved central part (inset of Fig. 4(b)). The spectrum also exhibits a complex structure on top of both edges caused by accumulated nonlinearity.
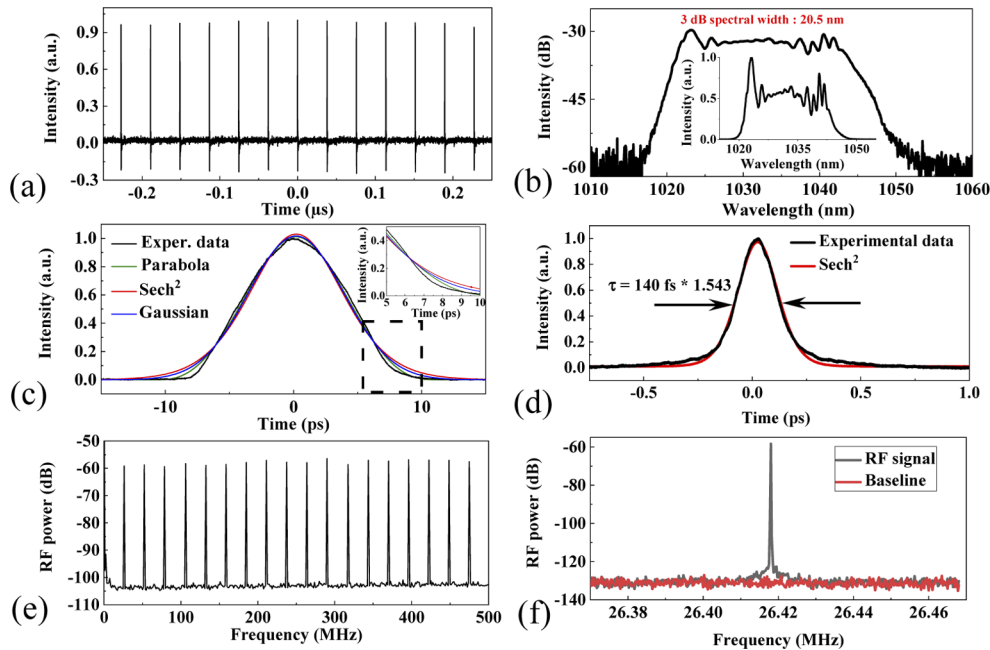
Fig. 4. Experimental laser performance: (a) pulse train and (b) spectrum. Inset of (b): spectrum in linear scale; Autocorrelation traces with fittings (c) before compression and (d) after compression. Green, blue and red lines correspond to parabolic, gaussian and hyperbolic ACF fittings. Inset of (c): Zoom-in view of framed part; RF spectra (e) in wide span of 500 MHz with resolution of 3 kHz and (f) in narrow span with 10 Hz resolution.

Autocorrelation traces are measured by second harmonic generation (SHG) based noncollinear autocorrelator and the results are shown in Fig. 4(c). For comparison, three fitting results by assuming pulse has parabolic, hyperbolic and Gaussian shapes are represented in Fig. 4(c). Corresponding coefficients of determination are 0.9981, 0.9917 and 0.9957, respectively, implying pulse shape is closer to parabola rather than other two typical pulse shapes. The retrieved pulse duration from parabolic autocorrelation function (ACF) fitting is 7.8 ps. A pair of 1250 line/mm diffraction gratings are subsequently used to externally compress pulse. Assuming compressed pulse has a hyperbolic shape, retrieved pulse has a duration of 140 fs, as shown in Fig. 4(d), leading to a time-bandwidth product of 0.808. Residual chirp is considered to stem from high order dispersion contributed by both fiber and grating pair. The autocorrelation trace of compressed pulse is clean and without oscillating pulse wings, providing further evidence of the near parabolic nature of the pulse from oscillator [8].

Radio frequency (RF) spectra in a wide span with 3 kHz resolution and in a narrow span with 10 Hz resolution are recorded and shown in Fig. 4(e) and Fig. 4(f), respectively. Nearly 70 dB signal to noise ratio at fundamental frequency of 26.4 MHz indicates stable mode-locking operation. The linewidth of RF spectrum is measured as narrow as 500 Hz indicating low jitter of the pulse. The bottom line coincides with the measurement device baseline indicating low-noise operation of this laser. The pulse-to-pulse fluctuation is estimated to be 1%. The stability of the laser operation has been confirmed by 2-hour continuous operation revealing no pulse or spectrum deterioration.

Since the laser operates in hybrid mode-locking scheme the individual function of each technique (NPR and FSF) in similariton pulse formation and evolution is difficult to identify. Therefore, we replaced AOTF by a bandpass filter and a polarizer in the cavity to "switched off"

FSF technique experimentally. By adjusting the position of PCs and playing with the pump power level we could not get any stable pulse operation. We address this to not large enough modulation depth of NPR in our cavity as essential for stable pulse operation in all-normal dispersion fiber lasers [33]. This indicates that FSF technique plays crucial role in stabilization of self-similar pulse evolution in the cavity whereas NPR most probably works to form an initial seed pulse. To gain an in-depth understanding of the pulse dynamics in the cavity we performed numerical simulations.

5. Numerical simulation

To investigate the mechanism of similariton formation in the cavity with hybrid mode-locking we performed numerical simulations. Two-component generalized nonlinear Schrödinger equation (GNLSE) equation was solved using split-step Fourier method to simulate light propagation in fiber [34]:

$$\frac{\partial A_j}{\partial z} - i\frac{\beta_2}{2}\frac{\partial^2 A_j}{\partial t^2} - i\gamma\left(|A_j|^2 + \frac{2}{3}|A_{3-j}|^2\right)A_j - \frac{i}{3}\gamma A_j^* A_{3-j}^2 = \frac{g}{2}\left(A_j + \Omega_g^2\frac{\partial^2 A_j}{\partial t^2}\right), \quad j = 1, 2. \quad (1)$$

where β_2 is group velocity dispersion (GVD), γ is Kerr nonlinearity coefficient, g is saturated gain coefficient, which is assumed to be zero in single mode fiber (SMF). In active fiber, gain is simulated using the following equation:

$$g(z,t) = g(z) = g_0\left(1 + \frac{\int_0^{\tau_{win}}(|A_1(z,t)|^2 + |A_2(z,t)|^2)dt}{E_g}\right)^{-1}, \quad (2)$$

where g_0 is small signal gain, E_g is saturation energy and τ_{win} is simulation window size. The peak gain is set at 1030 nm. Parameter $\Omega_g = 33.3$ ps^{-1} (corresponding to ~ 20 nm) determines the width of the gain line. Length of active fiber and passive fiber are 1.25 m and 5 m, respectively. Time window is set as 36 ps, consisting of 1024 time points.

The modelling of lumped resonator elements was carried out using transfer functions $A' = A \cdot T$, where A is light field before element and A' is light field after element. Transfer function of output coupler includes all losses in the cavity: $T_o = 0.3$ (i.e. accumulated loss is 91%). Transfer functions of the polarizer and PCs are modelled using Jones matrices

$$T_{pol} = \begin{pmatrix} 1 & 0 \\ 0 & 0 \end{pmatrix}, \quad T_{PC} = \begin{pmatrix} \cos\theta & -\sin\theta \\ \sin\theta & \cos\theta exp(i\varphi) \end{pmatrix}.$$

where θ is angle of polarization rotation by the PCs and φ is phase delay between two polarization components introduced by polarization controller. $T_f = \frac{exp(-\omega^2)}{2\Omega_f^2}$ is used to model Gaussian filter transfer function, where Ω_f is filter width and $\Omega_f \approx \frac{2\pi\nu_{FWHM}}{1.665}$, ν_{FWHM} is the half-maximum filter bandwidth in frequency domain. Frequency shift is modelled as $\hat{A}'(\omega) = \hat{A}'(\omega + \Delta\omega)$, where $\Delta\omega$ is multiple of frequency grid size dw ($\sim$14 GHz). The values of parameters used in the simulation are summarized in Table 1. A Gaussian noisy pulse with low amplitude is used as input signal.

In absence of a frequency shift, this numerical scheme describes a similariton-type laser with NPR mode-locking technique, where at certain values of θ and φ a pulse with shape close to the parabola at the output is generated [30]. First, we test the effectiveness of FSF mode-locking in this scheme. This is done in two steps: 1) mode-locked operation with NPR "off"; 2) hybrid mode-locking including both techniques of NPR and FSF. By setting the value $\theta = 0$, NPR effect is excluded. Using random noise as input, 1000 circulations are simulated in cavity. It turns out that only when frequency shift is larger than 500 GHz mode-locked pulses can be obtained. At a

Table 1. Parameters used in simulation

Parameter	Value	Parameter	Value
γ (W^{-1} m^{-1})	0.00275	E_g (nJ)	0.69
β_2 (ps^{2}m^{-1})	0.0275	g_0 (m^{-1})	10
Ω_f (ps^{-1})	3.3 (~2 nm)	Ω_g (ps^{-1})	33.3 (~ 20 nm)

lower frequency shift, mode-locking does not occur. Since the value of frequency shift clearly did not correspond to the experimental data (69 MHz), we conclude that only FSF mode-locking is not capable of maintaining a similariton operation regime.

Then, we simulated the laser with hybrid mode-locking technique. Setting $\theta = 0.397\ \pi$, $\varphi = -0.142\pi$ and frequency shift at the minimum possible value determined by simulation grid parameters, pulse with a maximum spectral width of ~ 21 nm and a FWHM duration of about 8 ps is obtained. Its evolution in the resonator is shown in Fig. 5. After AOTF, which incorporates a polarizer, frequency shifter and bandpass filter, the pulse possesses a Gaussian-like shape with relatively low energy distributed along only one polarization axis and a narrow spectrum width. During propagation in the gain fiber, the pulse is amplified while its profile approaches a parabolic shape with a broad spectrum due to the action of self-phase modulation. Polarization controller distributes the energy between two orthogonal polarizations. Propagation of the pulse in the SMF further broadens the pulse duration and spectrum due to self- and cross-phase modulations. The action of the NPR results in change of energy distribution along the polarization axes. At the position of the output coupler, ~8-ps pulse with 21 nm spectral width is coupled out.
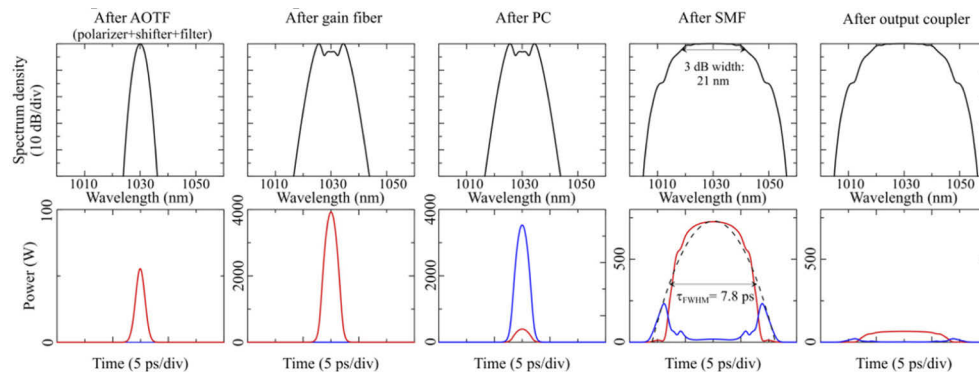

Fig. 5. Simulation results. Top row is the spectrum evolution. Bottom row is pulse evolution for two orthogonal polarizations. For comparison, the envelope of a parabolic pulse with a duration at half maximum of 7.8 ps is shown.

6. Conclusion

We demonstrate a similariton operation in an Yb-doped fiber laser with hybrid mode-locking technique incorporating nonlinear polarization rotation and frequency shifting techniques. The laser oscillator delivers 7.8 ps pulse with 20.5 nm spectrum and can be further compressed down to 140 fs. The study based on numerical simulation and experimental results revealed that employment of hybrid mode-locking for similariton-type lasers brings an additional pulse stabilization mechanism to the cavity by means of efficient filtering of low-intensity instabilities. This opens another route towards industry-grade similariton lasers with suppressed sensitivity to environmental perturbations.

Disclosures. X. L.: Tampere University (P), R. G.: Tampere University (P).

Data availability. The data underlying the results presented herein are not publicly available currently but can be obtained from the authors upon reasonable request.

References

1. R. Camassa, J. M. Hyman, and B. P. Luce, "Nonlinear waves and solitons in physical systems," Phys. D **123**(1-4), 1–20 (1998).
2. P. L. Christiansen, J. C. Eilbeck, and R. D Parmentier, *Future Directions of Nonlinear Dynamics in Physical and Biological Systems* (Springer Science & Business Media, 2013, Vol. 312).
3. A. Hasegawa and F. Tappert, "Transmission of stationary nonlinear optical pulses in dispersive dielectric fibers. I. Anomalous dispersion," Appl. Phys. Lett. **23**(3), 142–144 (1973).
4. N. J. Smith, F. M. Knox, N. J. Doran, K. J. Blow, and I. Bennion, "Enhanced power solitons in optical fibres with periodic dispersion management," Electron. Lett. **32**(1), 54–55 (1996).
5. E. V. Vanin, A. I. Korytin, A. M. Sergeev, D. Anderson, M. Lisak, and L. Vázquez, "Dissipative optical solitons," Phys. Rev. A **49**(4), 2806–2811 (1994).
6. X. Li, S. Zhang, and Z. Yang, "Optimal design of similariton fiber lasers without gain-bandwidth limitation," Opt. Express **25**(15), 18410–18420 (2017).
7. J. Zweck and C. R. Menyuk, "Computation of the timing jitter, phase jitter, and linewidth of a similariton laser," J. Opt. Soc. Am. B **35**(5), 1200–1210 (2018).
8. Youwen Jia, "Properties of mode-locked ultrafast fiber lasers," In *IOP Conf. Ser.: Mater. Sci. Eng.*, vol. 711, no. 1, p. 012103. IOP Publishing, (2020).
9. A. Chong, L. G. Wright, and F. W. Wise, "Ultrafast fiber lasers based on self-similar pulse evolution: a review of current progress," Rep. Prog. Phys. **78**(11), 113901 (2015).
10. C. Ma, A. Khanolkar, and A. Chong, "High-performance tunable, self-similar fiber laser," Opt. Lett. **44**(5), 1234–1236 (2019).
11. U. Teğin, E. Kakkava, B. Rahmani, D. Psaltis, and C. Moser, "Spatiotemporal self-similar fiber laser," Optica **6**(11), 1412–1415 (2019).
12. M. E. Fermann, V. I. Kruglov, B. C. Thomsen, J. M. Dudley, and J. D. Harvey, "Self-similar propagation and amplification of parabolic pulses in optical fibers," Phys. Rev. Lett. **84**(26), 6010–6013 (2000).
13. D. Anderson, M. Desaix, M. Karlsson, M. Lisak, and M. L. Quiroga-Teixeiro, "Wave-breaking-free pulses in nonlinear-optical fibers," J. Opt. Soc. Am. B **10**(7), 1185–1190 (1993).
14. B. Oktem, C. Ülgüdür, and F. Ilday, "Soliton–similariton fibre laser," Nat. Photonics **4**(5), 307–311 (2010).
15. Z. Wang, L. Zhan, X. Fang, and H. Luo, "Spectral filtering effect on mode-locking regimes transition: similariton-dissipative soliton fiber laser," J. Opt. Soc. Am. B **34**(11), 2325–2333 (2017).
16. C. Ma, A. Khanolkar, Y. Zang, and A. Chong, "Ultrabroadband, few-cycle pulses directly from a Mamyshev fiber oscillator," Photonics Res. **8**(1), 65–69 (2020).
17. A. Komarov, H. Leblond, and F. Sanchez, "Theoretical analysis of the operating regime of a passively-mode-locked fiber laser through nonlinear polarization rotation," Phys. Rev. A **72**(6), 063811 (2005).
18. C.-J. Chen, P. K. A. Wai, and C. R. Menyuk, "Soliton fiber ring laser," Opt. Lett. **17**(6), 417–419 (1992).
19. H. Sabert and E. Brinkmeyer, "Pulse generation in fiber lasers with frequency shifted feedback," J. Lightwave Technol. **12**(8), 1360–1368 (1994).
20. L. F. Mollenauer, J. P. Gordon, and S. G. Evangelides, "The sliding-frequency guiding filter: an improved form of soliton jitter control," Opt. Lett. **17**(22), 1575–1577 (1992).
21. Y. Kodama and S. Wabnitz, "Reduction and suppression of soliton interactions by bandpass filters," Opt. Lett. **18**(16), 1311–1313 (1993).
22. C. Martijn de Sterke and M. J. Steel, "Simple model for pulse formation in lasers with a frequency-shifting element and nonlinearity," Opt. Commun. **117**(5-6), 469–474 (1995).
23. G. Bonnet, S. Balle, T. Kraft, and K. Bergmann, "Dynamics and self-modelocking of a titanium-sapphire laser with intracavity frequency shifted feedback," Opt. Commun. **123**(4-6), 790–800 (1996).
24. R. Gumenyuk, D. A. Korobko, I. O. Zolotovsky, and O. G. Okhotnikov, "Role of cavity dispersion on soliton grouping in a fiber lasers," Opt. Express **22**(2), 1896–1905 (2014).
25. R. Gumenyuk, E. O. Okhotnikova, V. Filippov, D. A. Korobko, I. O. Zolotovskii, and M. Guina, "Fiber lasers of Prof. Okhotnikov: review of the main achievements and breakthrough technologies," IEEE J. Sel. Top. Quantum Electron. **24**(3), 1–14 (2018).
26. W. H. Renninger, A. Chong, and F. W. Wise, "Area theorem and energy quantization for dissipative optical solitons," J. Opt. Soc. Am. B **27**(10), 1978–1982 (2010).
27. A. Chong, W. H. Renninger, and F. W. Wise, "Properties of normal-dispersion femtosecond fiber lasers," J. Opt. Soc. Am. B **25**(2), 140–148 (2008).
28. M. Romagnoli, S. Wabnitz, P. Franco, M. Midrio, F. Fontana, and G. E. Town, "Tunable erbium–ytterbium fiber sliding-frequency soliton laser," J. Opt. Soc. Am. B **12**(1), 72–76 (1995).

29. M. W. Phillips, G. Y. Liang, and J. R. M. Barr, "Frequency comb generation and pulsed operation in a Nd: YLF laser with frequency-shifted feedback," Opt. Commun. **100**(5-6), 473–478 (1993).
30. William H. Renninger, Andy Chong, and Frank W. Wise, "Self-similar pulse evolution in an all-normal-dispersion laser," Phys. Rev. A **82**(2), 021805 (2010).
31. R. Dixon, "Acoustic diffraction of light in anisotropic media," IEEE J. Quantum Electron. **3**(2), 021805 (1967).
32. S. Boscolo, S. K. Turitsyn, and C. Finot, "Amplifier similariton fiber laser with nonlinear spectral compression," Opt. Lett. **37**(21), 4531–4533 (2012).
33. J. Jeon, J. Lee, and J. H. Lee, "Numerical study on the minimum modulation depth of a saturable absorber for stable fiber laser mode locking," J. Opt. Soc. Am. B **32**(1), 31–37 (2015).
34. R. V. Gumenyuk, D. A. Korobko, and I. O. Zolotovskii, "Stabilization of passive harmonic mode locking in a fiber ring laser," Opt. Lett. **45**(1), 184–187 (2020).